



**HAL**  
open science

# Interaction of Mo(CO)<sub>6</sub> and its derivative fragments with the Cu(001) surface: Influence on the decomposition process

Céline Dupont, Xiaowen Wan, Mikhail Petukhov, Peter Krüger

► **To cite this version:**

Céline Dupont, Xiaowen Wan, Mikhail Petukhov, Peter Krüger. Interaction of Mo(CO)<sub>6</sub> and its derivative fragments with the Cu(001) surface: Influence on the decomposition process. *International Journal of Quantum Chemistry*, 2014, 114 (23), pp.1630-1635. 10.1002/qua.24744 . hal-03555225

**HAL Id: hal-03555225**

**<https://hal.science/hal-03555225>**

Submitted on 3 Feb 2022

**HAL** is a multi-disciplinary open access archive for the deposit and dissemination of scientific research documents, whether they are published or not. The documents may come from teaching and research institutions in France or abroad, or from public or private research centers.

L'archive ouverte pluridisciplinaire **HAL**, est destinée au dépôt et à la diffusion de documents scientifiques de niveau recherche, publiés ou non, émanant des établissements d'enseignement et de recherche français ou étrangers, des laboratoires publics ou privés.

# Interaction of $\text{Mo}(\text{CO})_6$ and its derivative fragments with the $\text{Cu}(001)$ surface: influence on the decomposition process.

Céline Dupont<sup>\*†</sup>, Xiaowen Wan<sup>†</sup>, Mikhail Petukhov<sup>†</sup>, Peter Krüger<sup>†‡</sup>

July 7, 2014

## Abstract

A theoretical study on the adsorption and decomposition of molybdenum carbonyl on the copper (001) surface is reported. The adsorption structures and energies of  $\text{Mo}(\text{CO})_n$  molecules ( $n=1 \dots 6$ ) are computed systematically using Density Functional Theory (DFT) with Van der Waals corrections. By analyzing the energies of the various conformations, the main factors that determine the stable adsorption geometry are identified. Insight into the thermodynamics of decomposition is gained by calculating the reaction energy for dissociation of  $\text{Mo}(\text{CO})_n$  into  $\text{Mo}(\text{CO})_{n-1}$  and CO. In the gas phase, this reaction is highly endothermic for all  $n$ . On the Cu surface however, removal of the first CO group ( $n=6$ ) becomes strongly exothermic. The subsequent dissociation steps ( $n<6$ ), are endothermic even on the surface, but the reaction energies are much reduced. Dissociation is found energetically more favourable than desorption in all cases. The results clearly show that molybdenum carbonyl decomposition is strongly facilitated by the presence of the Cu surface.

---

\*celine.dupont@u-bourgogne.fr

†ICB, UMR 6303, University of Burgundy CNRS, 21078 Dijon, France.

‡Present address: Graduate School of Advanced Integration Science, Chiba University, Chiba 263-8522, Japan.

# INTRODUCTION

Metal carbonyls sublime at relatively low temperature and can be easily decomposed by ultra-violet light or electron beam irradiation. They are thus suitable for numerous applications through nano-controlled deposition techniques under vacuum conditions.<sup>1-4</sup> For example, the carbonyl deposits can be used either in microelectronics<sup>5,6</sup> or as supported metal catalysts.<sup>7-9</sup> It is thus important to understand the mechanisms governing adsorption, dissociation and desorption of the molecule. A number of experimental studies on the interaction of carbonyl species, especially  $\text{Mo}(\text{CO})_6$ , with different surfaces have been reported in the literature. It has been demonstrated that for low exposures on a clean  $\text{Rh}(100)$  surface at 80 K,  $\text{Mo}(\text{CO})_6$  molecules adsorb dissociatively into fragments until the first monolayer is formed.<sup>10</sup> On most noble metals, metal oxides and relatively inert surfaces, in contrast,  $\text{Mo}(\text{CO})_6$  physisorbs at liquid-nitrogen temperature and desorbs upon thermal heating to 200 K.<sup>11-15</sup> Adsorption of entire  $\text{Mo}(\text{CO})_6$  molecules has been reported for  $\text{Si}(111)$ ,  $\text{Ag}(111)$ ,  $\text{Pt}(111)$ ,  $\text{Cu}(111)$  and graphite. In the case of  $\text{Cu}(111)$ , competition between desorption and dissociation was observed in the monolayer range, at temperatures approaching the desorption point (200K).<sup>11</sup> Decomposition of the molecules upon continued scanning has also been evidenced.<sup>16</sup>

In our previous works,<sup>15,16</sup> we have focused on the structure of dense monolayers adsorbed on  $\text{Cu}(111)$ . The  $\text{Cu}(001)$  surface is also very interesting for deposition applications, because being slightly less stable than  $\text{Cu}(111)$ , it can be expected to have a somewhat enhanced reactivity. For the question of what controls the competition between adsorption and decomposition it is important to understand the interaction of a single  $\text{Mo}(\text{CO})_6$  molecule and its decomposition products  $\text{Mo}(\text{CO})_n$  ( $n = 1 \dots 5$ ) with the substrate. To this end reliable values for the reaction energies are required for every step of molybdenum carbonyl decomposition on the surface.

In this work we have used density functional theory (DFT) to compute the structure and energetics of the molybdenum hexa-carbonyl molecule and its fragments ( $\text{Mo}(\text{CO})_n$ ,  $n = 1 \dots 5$ ) on  $\text{Cu}(001)$ . The possible conformations of each species have been studied systematically

both in the gas phase and on the Cu surface. Their adsorption geometries are described and their dissociation and adsorption energies are compared, providing insights into the decomposition process.

## METHODOLOGY

The adsorption of a  $\text{Mo}(\text{CO})_6$  molecule on  $\text{Cu}(001)$  as well as its decomposition fragments  $\text{Mo}(\text{CO})_n$  ( $n = 1 \dots 5$ ) has been studied with density functional theory (DFT) in periodic boundary conditions. The calculations were performed with the VASP code<sup>17,18</sup> using the projector-augmented wave (PAW) method<sup>19</sup> and the Perdew-Burke-Ernzerhof<sup>20</sup> exchange-correlation functional. The plane-wave cutoff was set to 400 eV, and the Brillouin zone integrations were done on a  $(4 \times 4 \times 1)$  Monkhorst-Pack  $k$ -point mesh. A low threshold (0.01 eV. $\text{\AA}^{-1}$ ) was applied for the minimization of the residual forces during the geometry optimizations of all the stationary points. As entire hexacarbonyls tend to physisorb on many substrates, Van der Waals interactions must be taken into account when studying  $\text{Mo}(\text{CO})_6$  adsorption. Here pair-wise dispersion forces have been added to the DFT energy functional, by following the D2 scheme proposed by Grimme<sup>21</sup> with a cutoff radius of 15  $\text{\AA}$ . Spin-polarized calculations have been performed throughout the study. Substantial spin-polarization is found only for the gas phase molecules and their spin states are briefly discussed below.

A supercell approach has been employed for modeling the surface with periodic slabs of four  $\text{Cu}(001)$  layers separated by a vacuum of 16.6  $\text{\AA}$ , corresponding to almost 10 equivalent metallic layers. The two upper layers were allowed to relax, while the two lowest ones were frozen at their bulk like positions. The theoretical lattice parameter of 3.573  $\text{\AA}$ , is good agreement with the experimental value of 3.620  $\text{\AA}$ . Adsorption has been modeled with a single molecule in a  $5 \times 5$  supercell, *i.e.* a square with a side of 12.63  $\text{\AA}$ .

# RESULTS AND DISCUSSION

## Gas phase conformations

Before investigating  $\text{Mo}(\text{CO})_n$  adsorption on  $\text{Cu}(001)$ , the structure and energetics of  $\text{Mo}(\text{CO})_n$  molecules in the gas phase have been determined. The most stable conformations are represented in Figure 1. Other possible conformations have also been optimized, namely a linear shape for  $\text{Mo}(\text{CO})_2$ , a T-shape for  $\text{Mo}(\text{CO})_3$  and square planar shape for  $\text{Mo}(\text{CO})_4$ , but they have higher energies: from 0.55 eV for  $\text{Mo}(\text{CO})_2$  to 1.22 and 1.27 eV for  $\text{Mo}(\text{CO})_4$  and  $\text{Mo}(\text{CO})_3$ , respectively. Hence they will not be discussed further. In all structures, the CO ligands of the fragments are nearly at right angles, as for the saturated  $\text{Mo}(\text{CO})_6$  molecule with octahedral geometry. In the stable structures shown in Figure 1, all CO ligands point to neighboring corners of an octahedron, that is,  $\text{Mo}(\text{CO})_2$  is bent rather than straight, and  $\text{Mo}(\text{CO})_3$  and  $\text{Mo}(\text{CO})_4$  are 3-dimensional rather than planar. This means that, under the constraint of ligands pointing to the corners of an octahedron, the stable geometries are those where the average CO-CO distance is minimized. These specific geometries of the  $\text{Mo}(\text{CO})_n$  molecules have been attributed to the Mo-d and CO- $\pi/\pi^*$  orbitals interaction.<sup>22-24</sup> The present results are in good agreement with the experimental and theoretical literature.<sup>25</sup>

## Mo adsorption

As a preliminary study for the  $\text{Mo}(\text{CO})_n$  adsorption, it is useful to consider the adsorption of atomic molybdenum. Its adsorption was investigated in top, bridge and hollow positions. The bridge position is unstable and its optimization converged to the hollow site. The optimized structures of top and hollow sites are shown in Figure 2. The hollow site clearly ( $E_{ads} = -2.60$  eV) is much more stable than the top site ( $E_{ads} = -1.59$  eV) as expected because of the four times larger coordination. Interestingly, on-top adsorption would lead to a large surface deformation around the Mo atom as seen in Figure 2. The nearest neighbor Cu atom relaxes into the bulk by 0.71 Å while the four next nearest neighbor Cu atoms move outwards by 0.16 Å. The Cu-Cu distance is thereby substantially reduced resulting in an

effective increase of Mo-Cu coordination.

## Mo(CO) $_n$ adsorption

First we consider adsorption of the Mo(CO) $_6$  molecule. This saturated, octahedral molecule cannot form direct Mo-Cu or C-Cu bonds, for both steric and electronic reasons. Instead, Mo(CO) $_6$  interacts with Cu surfaces by Van der Waals forces only, as it was previously shown for the Cu(111) substrate<sup>15</sup>. It has a low adsorption energy of -0.39 eV on the Cu(001), similar to the one calculated on Cu(111) (-0.44 eV).<sup>15</sup>

We now turn to the fragments Mo(CO) $_n$  with  $n = 1 \dots 5$ . From the results on single atom Mo adsorption, one may expect that hollow site adsorption is also preferred for the Mo(CO) $_n$  fragments. To check this, tests have been performed for several Mo(CO) $_n$  fragments with Mo either at on-top, bridge or hollow position. In all cases, the hollow site was found most stable. We therefore limit the following discussion to fragments with Mo at on-top sites. Apart from this restriction, all possible conformations of Mo(CO) $_n$  on the surface have been considered. For the classification of the different structures, we first count the number of CO ligands that are directly bonded to the surface. Second we distinguish CO at on-top and bridge sites. Because the CO ligands are (nearly) orthogonal, either all CO ligands are at on-top or all are at bridge sites. A specific notation, namely  $X_a^b$ , is used to properly describe the adsorbed Mo(CO) $_n$ , ( $n = 1 \dots 5$ ).  $X$  refers to the adsorption site of the CO ligands with  $X=T$  for top and  $X=B$  for bridge site.  $a$  gives the number of CO ligands directly bonded to the surface.  $b$  refers to the structure of the fragment:  $G$  indicates that the gas conformation is preserved,  $NG$  that a different structure is considered. All possible configurations have been studied systematically. The various optimized structures of Mo(CO) $_n$ /Cu(001) are represented in Figure 3 and their adsorption energies are reported in Table 1.

Mo(CO) $_2$  is the only fragment that presents all possible conformations. It is thus best suited to discuss the role of the various structural parameters ( $X_a^b$ ) for the stability of the conformation. From the adsorption energies (Table 1), it can be seen that, when both CO are adsorbed on the surface, the gas phase conformation is most stable. Hence the  $T_2^{NG}$

structure is 0.44 eV less stable than the  $T_2^G$  one, while a gap of 0.60 eV is observed between the two bridge structures,  $B_2^{NG}$  and  $B_2^G$ , respectively. This difference of stability is of the same order of magnitude as the one observed in gas phase (0.55 eV, as mentioned previously), ruling out a specific role of the surface.

For the two conformations corresponding to the gas phase structure, the influence of the numbers of ligands bound to the surface can now be investigated. It appears that the more CO groups are bound to the surface, the higher is the adsorption energy. Nevertheless, this point has less influence than the structure of the fragment, as a difference of only 0.31 eV is observed between the top structures  $T_2^G$  and  $T_1^G$ , 0.19 eV between the bridge ones ( $B_2^G$  and  $B_1^G$ ). Last, it can be seen that the orientation of the CO ligands (top versus bridge) has the least influence:  $T_2^G$  and  $B_2^G$  differ by only 0.1 eV. This low influence of the CO orientation is directly related to the nature of CO-Cu interaction. In the  $\text{Mo}(\text{CO})_n$ , the CO ligands do not stand vertically over the surface, as can be seen in Figure 3, contrary to an isolated CO molecule adsorbed. Therefore the orbital interaction usually involved in the CO adsorption cannot occur: the interaction between the CO ligands and the metallic surface is now mainly due to dispersion. Therefore the relative stability of the bridge or the top orientation will not be discussed further.

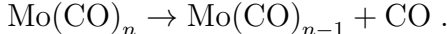
In conclusion, the adsorption of  $\text{Mo}(\text{CO})_2$  is mainly governed by the proximity of the two CO ligands, which implies adopting the same conformation as in the free molecules. The second factor is the CO-Cu stabilizing interaction which maximizes the number of CO on the surface.

These two rules are respected for all other fragments. Results for  $\text{Mo}(\text{CO})_3$  and  $\text{Mo}(\text{CO})_4$  confirm that keeping the gas phase structure is the main element governing the stability of a conformation. Hence for these two fragments, the  $X_{n-1}^G$  conformations (and even  $X_{n-2}^G$  for  $\text{Mo}(\text{CO})_4$ ) are always more stable than the  $X_n^{NG}$  ones. Next, the importance of the bonds between the surface and the CO ligands is also confirmed. For example, different attempts have been made to stabilize  $T_1^G$  and  $B_1^G$ , but all these calculations have evolved to  $X_2^G$  structures. This tendency is also verified for  $\text{Mo}(\text{CO})_1$ : the  $X_0^G$  structure with no CO-Cu interaction is the least stable, followed by  $T_1^G$  and  $B_1^G$ , with the CO on top and the CO on bridge position, respectively.

Hence for all fragments, the structure with the gas phase conformation and with the maximum number of CO groups bonded to the surface is always the most stable one.

## Dissociation

Based on these adsorption results, the thermodynamic aspects of the  $\text{Mo}(\text{CO})_6$  dissociation are considered. Molybdenum carbonyl dissociates by successively losing CO ligands according to the reaction



Dissociation on the copper surface will be compared to the dissociation in gas phase. In this framework, the dissociation energy of a  $\text{Mo}(\text{CO})_n$  fragment in gas phase is defined as

$$E_{dis}(n, g) = E(\text{Mo}(\text{CO})_{n-1}, g) + E(\text{CO}, g) - E(\text{Mo}(\text{CO})_n, g) ,$$

where  $E(\text{Mo}(\text{CO})_n, g)$  is the energy of the  $\text{Mo}(\text{CO})_n$  fragment in gas phase.

For the dissociation of the adsorbed molecules we consider a final state where both the  $\text{Mo}(\text{CO})_{n-1}$  fragment and the CO molecule stay on the surface. We also assume that  $\text{Mo}(\text{CO})_{n-1}$  and CO are sufficiently separated so that their interaction energy can be neglected. Under these assumptions, the dissociation energy of  $\text{Mo}(\text{CO})_n$  on the surface is given by

$$E_{dis}(n, S) = E(\text{Mo}(\text{CO})_{n-1}/S) - E(\text{Mo}(\text{CO})_n/S) + E(\text{CO}, g) + E_{ads}(\text{CO}) ,$$

where  $E(\text{Mo}(\text{CO})_n/S)$  is the energy of the  $\text{Mo}(\text{CO})_n$  fragment adsorbed on the Cu slab and  $E_{ads}(\text{CO}) = E(\text{CO}/S) - E(\text{CO}, g) - E(S)$  is the adsorption energy (-1.18 eV) of a single CO molecule on Cu(001) at the hollow site. On-top and bridge sites were found slightly less stable with adsorption energies of -1.06 and -1.14 eV, respectively.

Following these equations, dissociation energies are calculated for molecules in gas phase and adsorbed on Cu(001) and are reported in Table 2.

Dissociation of  $\text{Mo}(\text{CO})_6$  down to  $\text{Mo}(\text{CO})_3$  has already been investigated in gas phase both theoretically<sup>25,26</sup> and experimentally.<sup>27,28</sup> These studies have led to dissociation energies between 1.3 and 1.75 eV for the first three steps ( $n = 6, 5, 4$ ). The corresponding dissociation



energies obtained in this work are close to 1.85 eV, and are thus fully consistent with the literature. According to our results, a break point appears for the dissociation of  $\text{Mo}(\text{CO})_3$ , which has a high energy of 3.05 eV. This can be directly related to the spin state transition during the dissociation process: while species from  $\text{Mo}(\text{CO})_6$  to  $\text{Mo}(\text{CO})_3$  are singlet,<sup>25</sup>  $\text{Mo}(\text{CO})_2$ ,  $\text{Mo}(\text{CO})_1$  and Mo are all septet.<sup>29,30</sup> Hence, when a CO ligand is removed from  $\text{Mo}(\text{CO})_3$  the system undergoes a low to high spin transition which gives rise to a large dissociation energy.

The comparison of the dissociation energies in gas phase with those at the Cu(001) surface clearly demonstrates that the surface plays an essential role in activating the dissociation. Indeed, while all elementary dissociation steps are endothermic in the gas phase, the first step is highly exothermic (-2.10 eV) on the metal. This first exothermic step will initiate the dissociation process at the surface. Then, even though the following dissociations are endothermic, the presence of the surface significantly lowers the reaction energy of each step. Taking into account the high adsorption energies calculated for the different fragments, the desorption of the  $\text{Mo}(\text{CO})_n$  ( $n=1 \dots 5$ ) species seems unlikely. To confirm this point, the competition between desorption and dissociation is analyzed through the value of  $\Delta$  defined as the difference between the desorption energy and the dissociation energy:  $\Delta = E_{des} - E_{dis}$ , where  $E_{des} = -E_{ads}$ . Dissociation energies in gas phase and on the Cu(001) surface, as well as  $\Delta$  values are reported in Table 2. It can be seen that  $\Delta$  is large and positive in all cases, which implies that dissociation will always be favored over desorption, at least from a purely thermodynamic point of view. Despite the differences in absolute energies between the gas phase and on the copper surface, it appears that  $\text{Mo}(\text{CO})_3$  plays a specific role not only in the gas phase but also on the surface. We have  $\Delta = 2.08$  eV for  $\text{Mo}(\text{CO})_3$ , but much larger values ( $> 2.5$  eV), for all other fragments. This means that the energetic preference for dissociation over desorption is less pronounced for  $\text{Mo}(\text{CO})_3$  than for the other fragments. This results also suggests that, if the sequence of dissociation stops, this will probably happens at the  $\text{Mo}(\text{CO})_3$  fragment.

## CONCLUSIONS

Adsorption and dissociation of molybdenum hexacarbonyl on the Cu(001) surface have been studied from first principles calculations. The entire  $\text{Mo}(\text{CO})_6$  molecule interacts with the Cu(001) surface through Van der Waals forces. Adsorption of all  $\text{Mo}(\text{CO})_n$  fragments ( $n=1..5$ ) has been analyzed systematically, revealing the main factors governing the adsorption geometry. The first point is the metallic Mo-Cu bonding, since in all cases the Mo atom is directly bonded to Cu at hollow adsorption sites. The second factor is the relative position of the CO ligands. The ligands always arrange to be orthogonal to each other when possible and thus occupy neighboring sites in octahedral coordination, as it is the case in the gas phase. Finally there is an attractive CO-Cu interaction, which orients the fragments at the surface such that a maximum number of CO ligands can interact with the copper atoms. Next, molybdenum carbonyl dissociation has been investigated through a purely thermodynamic approach. It is found that the presence of the copper surface has a major effect on the dissociation energetics. In the gas phase, each dissociation step from  $\text{Mo}(\text{CO})_6$  to Mo, by subsequent loss of a CO ligand, is a highly endothermic process. At the Cu(001) surface, however, the loss of the first CO becomes exothermic and the reaction energies of all following steps are strongly reduced from the gas phase values, showing that  $\text{Mo}(\text{CO})_6$  dissociation is greatly facilitated by the surface. The comparison between desorption and dissociation energies indicates, from a thermodynamic point of view, that  $\text{Mo}(\text{CO})_3$  is the fragment that is most likely to remain at the surface after partial dissociation of  $\text{Mo}(\text{CO})_6$ . However, further studies on the activation energies of each elementary process are required to confirm this conclusion by including the kinetic aspects of the problem.

## References

1. C. Cho and S. Bernasek, *J. Appl. Phys.* **65**, 3035 (1989).
2. M. Walz, M. Schirmer, F. Vollnhals, T. Lukasczyk, and H. Steinrück, *Angew. Chem. Int. Ed.* **49**, 4669 (2010).
3. W. Chang, S. Bauerdick, and M. Jeong, *Ultramicroscopy* **108**, 1070 (2008).
4. P. Väterlein, V. Wüstenhagen, and E. Umbach, *Appl. Phys. Lett.* **66**, 2200 (1995).
5. D. Bäuerle, *Chemical Processing with Lasers* (Springer, Berlin, 1986).
6. D. J. Ehrlich and J. Y. Tsao, *Laser Microfabrication, Thin Film Processes and Lithography* (Academic, San Diego, 1989).
7. M. B. Logan, R. F. Howe, and R. P. Cooney, *J. Mol. Cat.* **74**, 285 (1992).
8. S. D. Djajanti and R. F. Howe, *Stud. Surf. Sci. Catal.* **97**, 197 (1995).
9. Z. Q. Jiang, W. X. Huang, J. Jiao, H. Zhao, D. L. Tan, R. S. Zhai, and X. H. Bao, *App. Surf. Sci.* **229**, 43 (2004).
10. T. Germer and W. Ho, *J. Chem. Phys.* **89**, 562 (1988).
11. Z. Ying and W. Ho, *J. Chem. Phys.* **93**, 9077 (1990).
12. S. So and W. Ho, *J. Chem. Phys.* **95**, 656 (1991).
13. J. Evans, B. Hayden, and G. Lu, *Chem. Soc., Faraday Trans.* **92**, 4733 (1996).
14. C. Yeh, Y. Lai, W. Chu, C. Yeh, and W. Hung, *Surf. Sci.* **565**, 81 (2004).
15. P. Krüger, M. Petukhov, B. Domenichini, A. Berkò, and S. Bourgeois, *J. Phys. Chem. C* **116**, 10617 (2012).
16. M. Petukhov, P. Krüger, B. Domenichini, and S. Bourgeois, *Surf. Sci.* **617**, 10 (2013).
17. G. Kresse and J. Hafner, *Phys. Rev. B* **47**, 558 (1993).

18. G. Kresse and J. Furthmüller, Phys. Rev. B **54**, 11169 (1996).
19. G. Kresse and D. Joubert, Phys. Rev. B **59**, 1758 (1999).
20. J. P. Perdew, K. Burke, and M. Ernzerhof, Phys. Rev. Lett. **77**, 3865 (1996).
21. S. Grimme, J. Comput. Chem. **27**, 1787 (2006).
22. P. J. Hay, J. Am. Chem. Soc. **100**, 2411 (1978).
23. J. Demuyne, E. Kochanski, and A. Veillard, J. Am. Chem. Soc. **101**, 3467 (1979).
24. L. A. Barnes, B. Liu, and R. Lindh, J. Chem. Phys. **98**, 3978 (1993).
25. Y. Ishikawa and K. Kawakami, J. Phys. Chem. A **111**, 9940 (2007).
26. A. Ehlers and G. Franking, J. Am. Chem. Soc. **116**, 1514 (1994).
27. M. Bernstein, J. Simon, and J. Peters, Chem. Phys. Lett. **100**, 241 (1983).
28. K. Lewis, D. Golden, and D. Smith, J. Am. Chem. Soc. **106**, 3905 (1984).
29. S. G. Wang, X. Y. Chen, and W. H. E. Schwarz, J. Chem. Phys. **126**, 124109 (2007).
30. H. Tan, M. Liao, D. Dai, and K. Balasubramanian, J. Phys. Chem. A **102**, 6801 (1998).

Figure 1: Optimized structures of the unsaturated fragments  $\text{Mo}(\text{CO})_n$  ( $n=1 \dots 5$ ) as well as the initial molecule  $\text{Mo}(\text{CO})_6$ , in gas phase. The following symmetry groups are observed,  $O_h$  for  $\text{Mo}(\text{CO})_6$ ,  $C_{4v}$  for  $\text{Mo}(\text{CO})_5$ ,  $C_{2v}$  for  $\text{Mo}(\text{CO})_4$ ,  $C_{3v}$  for  $\text{Mo}(\text{CO})_3$ ,  $C_{2v}$  for  $\text{Mo}(\text{CO})_2$  and  $C_{\infty v}$  for  $\text{Mo}(\text{CO})_1$ . Molybdenum atoms are represented in pink, carbon in gray and oxygen in red.

Figure 2: (A) Top and (B) lateral views for optimized structures of molybdenum chemisorption on  $\text{Cu}(001)$ . Adsorption on hollow position is reported on the left while top position is on the right. Copper atoms are represented in orange, molybdenum in pink. (C) Corresponding adsorption energies in eV.

Figure 3: Optimized structures for  $\text{Mo}(\text{CO})_n$  ( $n=1 \dots 6$ ) adsorption on  $\text{Cu}(001)$ . Top and lateral views are given for each stable conformation, labelled using the specific notation  $X_a^b$ , where X refers to the top (T) or bridge (B) position of adsorbed CO ligands,  $a$  indicates the number of CO ligands coordinated to the surface with  $n$  being the total number of ligands of the fragments and  $b$  corresponds the respect of the gas phase structure (G) or not (NG). The most stable conformations are indicated in bold face. Copper atoms are represented in orange, molybdenum in pink, carbon in gray and oxygen in red.

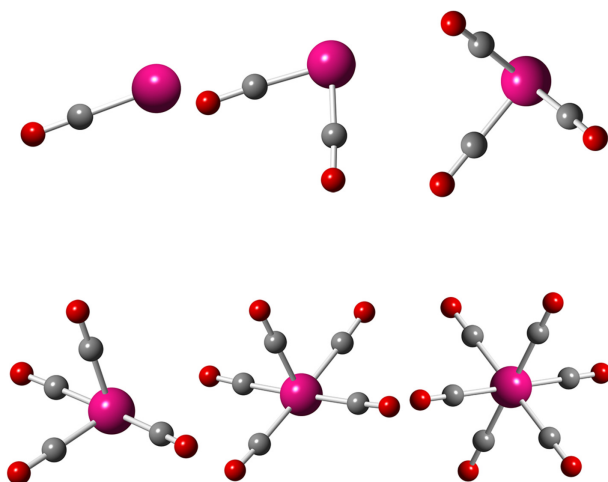


Figure 1  
C. Dupont, X. Wan, M.  
Petukhov, P. Krüger  
Int. J. Quant. Chem.

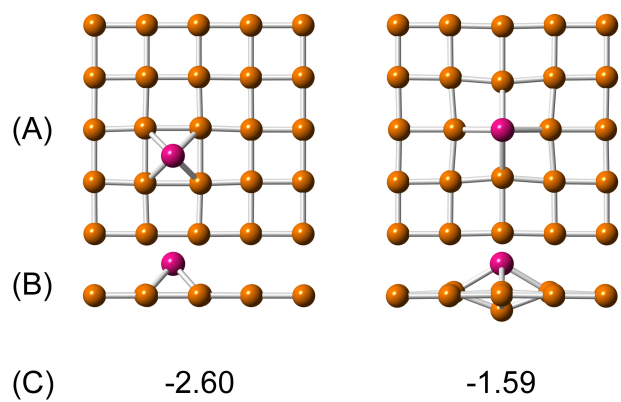


Figure 2  
 C. Dupont, X. Wan, M.  
 Petukhov, P. Krüger  
 Int. J. Quant. Chem.

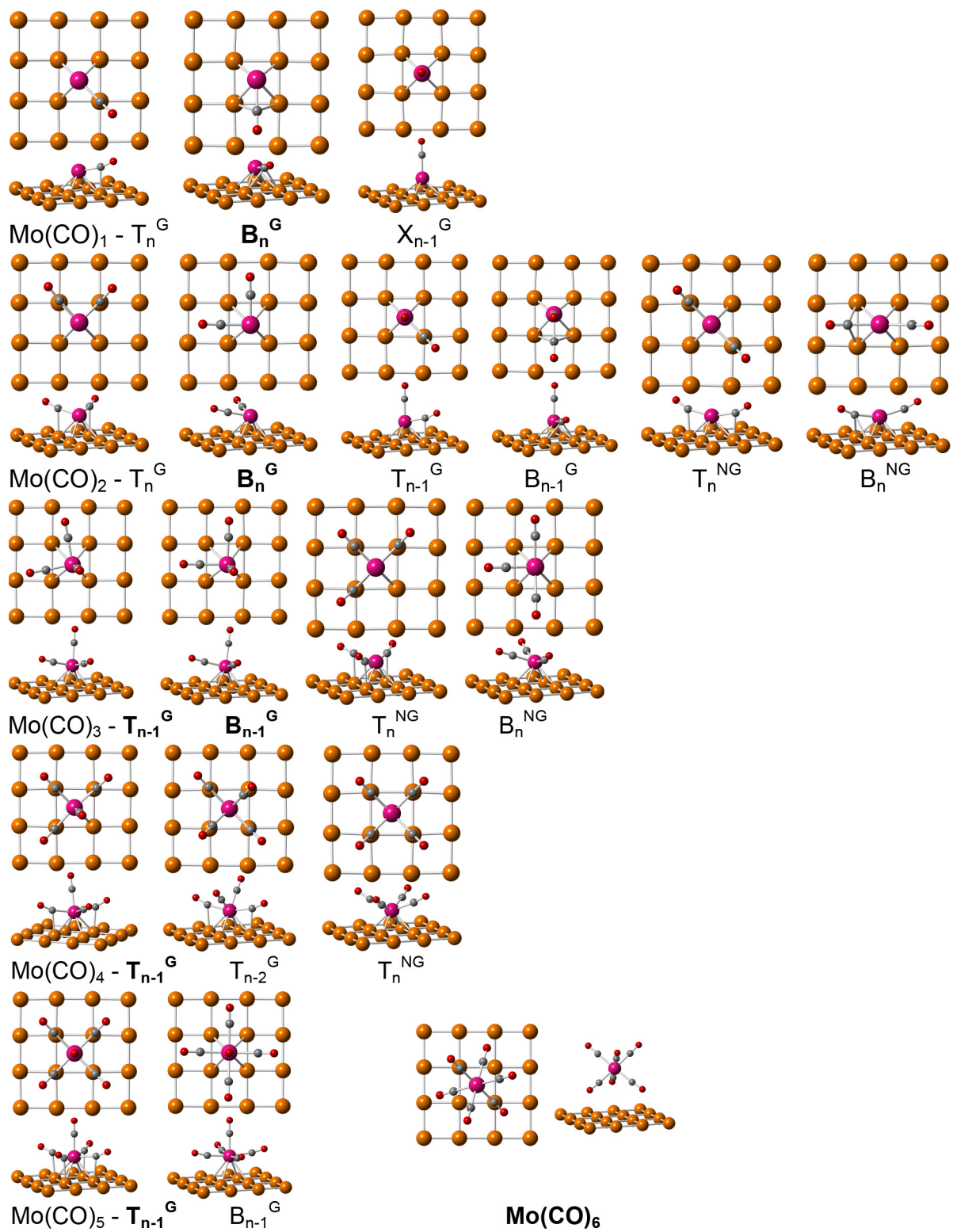




Figure 3  
C. Dupont, X. Wan, M.  
Petukhov, P. Krüger  
Int. J. Quant. Chem.

$\text{Mo}(\text{CO})_n$	$T_n^G$	$B_n^G$	$T_{n-1}^G$	$B_{n-1}^G$	$T_{n-2}^G$	$T_n^{NG}$	$B_n^{NG}$
$\text{Mo}(\text{CO})_1$	-3.74	-3.95	-3.49	-	-	-	-
$\text{Mo}(\text{CO})_2$	-3.86	-3.95	-3.56	-3.76	-	-3.42	-3.36
$\text{Mo}(\text{CO})_3$	-	-	-3.26	-3.26	-	-2.87	-2.74
$\text{Mo}(\text{CO})_4$	-	-	-3.29	-	-3.28	-2.95	-
$\text{Mo}(\text{CO})_5$	-	-	-3.17	-2.78	-	-	-
$\text{Mo}(\text{CO})_6$				-0.39			

Table 1: Adsorption energy ( $E_{ads}$ ) in eV for the different fragments  $\text{Mo}(\text{CO})_n$  ( $n=1\dots 6$ ). The specific notation ( $X_a^b$ ) defined in the text is used to name the different structures.

Reactant	Gas phase	Cu(001)	
	$E_{dis}$	$E_{dis}$	$\Delta$
$\text{Mo}(\text{CO})_6$	1.86	-2.10	2.49
$\text{Mo}(\text{CO})_5$	1.85	0.55	2.62
$\text{Mo}(\text{CO})_4$	1.90	0.74	2.55
$\text{Mo}(\text{CO})_3$	3.05	1.18	2.08
$\text{Mo}(\text{CO})_2$	2.39	1.21	2.74
$\text{Mo}(\text{CO})_1$	1.18	1.34	2.61

Table 2: Reaction energies ( $E_{dis}$ ) in eV for successive dissociations starting from  $\text{Mo}(\text{CO})_6$ . Each reaction energy corresponds to the loss of one CO ligand for the considered  $\text{Mo}(\text{CO})_n$  fragment. Values are given for dissociation in gas phase and on Cu(001). The competition on Cu(001) between desorption and dissociation is also reported through the value of  $\Delta$  (in eV) corresponding to  $E_{des}-E_{dis}$  where  $E_{des}$  is the desorption energy (defined as  $-E_{ads}$ ).